Neutral and charged thorium impurity in solid argon

A. V. Nikolaev [1,2,3] and E. V. Tkalya [4,2,5]

[1] *Skobeltsyn Institute of Nuclear Physics, Lomonosov Moscow State University, 119991 Moscow, Russia*

[2] *National Research Nuclear University MEPhI, Kashirskoe Shosse 31, 115409 Moscow, Russia*

[3] *School of Electronics, Photonics and Molecular Physics, Moscow Institute of Physics and Technology, Dolgoprudny, 141700 Moscow Region, Russia*

[4] *P.N. Lebedev Physical Institute of the Russian Academy of Sciences, 53 Leninskiy Prospekt, 119991 Moscow, Russia*

[5] *Nuclear Safety Institute of RAS, Bol'shaya Tulskaya 52, 115191 Moscow, Russia*

(Received 23 June 2021; revised 31 August 2021; accepted 14 September 2021; published 21 September 2021)

We study the neutral and positively charged thorium impurity (Th^{n+}, $n = 0, 1, 2, 3, 4$) in solid argon by exploring the nature of chemical bonding in the ThAr diatomic molecule and in clusters $ThAr_4$, $ThAr_{12}$, $Th^{n+}Ar_{18}$ at the Hartree-Fock level with the second-order perturbation (MP2) correction accounting for the van der Waals forces. The chemical bonding is formed from the valence states of thorium and polarized states of argon in the clusters with Th^{n+} ($n = 0, 1, 2, 3$) and solely from polarized states in the clusters with Th^{4+}. In all cases with two or more valence electrons of Th, the ground state, influenced by the first Hund rule for the thorium impurity, is the high spin state. Allowing for the cubic to orthorhombic (D_{2h}) symmetry lowering in $Th^{n+}Ar_{18}$, we find that the averaged Th-Ar bond length decreases whereas the binding energy increases with n, accounted for by the weakening of the Th-Ar repulsion and the strengthening of polarization. For $Th^{4+}Ar_{18}$, two conformations (cubic and orthorhombic) are found. We conclude that with the Th-Ar bond lengths lying very close to the Ar-Ar bond lengths in a fcc lattice, the solid argon is a material that is well suited for the accommodation of thorium impurities.

DOI: 10.1103/PhysRevA.104.032819

I. INTRODUCTION

Presently, the periodic table includes 118 chemical elements. Since each nucleus of these atoms can have a different number of neutrons, the total number of all known nuclides amounts to 3000 [1]. And out of this diversity, there is only a single nucleus which can be excited into a high state by absorbing the electromagnetic radiation of the wavelength as large as ∼150 nm, which is more typical for the atomic scale of energies. This nucleus is ^{229}Th, whose spectrum of excited states starts off from the level $3/2^+$ (8.19 ± 0.12 eV) [2–4].

First indications of the low-lying state in the ^{229}Th nucleus were given in Ref. [5] in 1976. At the beginning of the 1990s, it became clear that we are dealing with a unique doublet of nuclear levels separated with an energy gap of several electronvolts [6,7]. As a result of accurate experiments [3,4,8] performed after 2007, it has turned out that the energy of the nuclear transition lies in the ultraviolet range and approximately equals 8.2 eV.

Such an unusual nuclear transition has immediately drawn the attention of researchers from various fields of physics. The nuclear isomer ^{229m}Th ($3/2^+$, 8.2 eV) can be used as a sensitive probe for studying its chemical environment [9] or as a constituent part of the so-called electron bridge [9–16]—a process of excitation and decay of the nuclear state through the electron shell in the third order of the constant of the electromagnetic interaction e of the perturbation theory of quantum electrodynamics. There is a whole set of interesting effects predicted for ^{229m}Th, among which we mention the control of the decay of the nuclear isomer by means of boundary conditions [17], the investigation of the relative effects of the variation of the fine-structure constant and the strong interaction parameter [18–20], the decay of the ^{229}Th nuclear ground state to the isomeric level in the muon atom of thorium [21], the search of dark matter [22], the testing of the exponentiality of the basic decay law [23], the change of the velocity of the alpha decay of ^{229}Th through the isomer excitation by laser radiation [24], and others.

Most of the attention, however, is focused on possible technological applications of the unusual properties of ^{229m}Th: the metrological time standard (including the solid-state one) [25–28], the laser on the nuclear transition [29,30], and the nuclear light-emitting diode [31]. In dielectrics with a large gap of forbidden states (including solid argon), the ^{229m}Th level is expected to decay by emitting a photon with the half life of an hour. Therefore, the isomeric transition to the ground ^{229}Th state has an extremely narrow relative linewidth of $\delta E/E \sim 10^{-20}$. This makes ^{229m}Th a very promising candidate for constructing a nuclear frequency standard that can outperform today's most advanced optical atomic clocks ($\delta E/E \sim 10^{-18}$) and has the potential for further improvement. For the successful functioning of these devices, it is required that the $^{229m}\text{Th} \rightarrow {}^{229}\text{Th}$ nuclear transition results in photon emission. Unfortunately, the main channel of the decay of low-lying isomeric states is the internal conversion when the excess of the

nuclear energy is transferred to a bound electron which leaves the atomic shell and gets excited into a continuum state. At present, there are two principal ways to overcome this obstacle and achieve the radiative transition: laser-cooled trapped ^{229}Th ions and Th-doped solids [32,33], to which our study belongs. In the last case, ^{229m}Th is a substitutional impurity in a dielectric solid, and when the gap of the forbidden states exceeds the nuclear transition energy (8.2 eV), the conversion is not allowed and the ^{229m}Th isomer decays by emitting the γ quantum of the ultraviolet range.

At present, there are relatively few media known to satisfy this condition: Na_2ThF_6, $LiCaAlF_6$, $LiSrAlF_6$, $LiYF_4$, CaF_2 [26,34], SiO_2 [35], as well as matrices of frozen inert gases Ar, Ne, Xe, and Cr, used by Borisyuk's team at MEPhI [36]. All of them are thoroughly studied as materials which can potentially be used for creating nuclear clocks, the laser on nuclear transition, and the nuclear light-emitting diode. Experiments with thorium nuclei implanted in the most popular media—$LiCaAlF_6$ and $LiSrAlF_6$—are described, e.g., in [37].

In this work, we study in detail the properties of an isolated thorium impurity in a matrix of the frozen inert argon with the energy gap ~12 eV [38–40]. Our aim, therefore, is to discuss the possibility to use solid argon as an appropriate media for Th to enable its nuclear transition. In particular, we analyze the bonding characteristics and other physicochemical quantities of the neutral Th atom and thorium cations (Th^{n+}, $n = 1 - 4$) in solid argon clusters modeling argon matrices.

It is worth mentioning that solid argon, as with other rare gases (neon and krypton), is crystallized in the face-centered-cubic (fcc) structures at ambient pressure and low temperatures below the melting point at $T = 83.8$ K [41]. However, even at low temperatures, the fcc phase often coexists with the close-packed hexagonal (hcp) one [41]. The fcc-to-hcp transition in argon induced by applying external pressure above 49.6 GPa has been extensively studied both experimentally [42,43] and theoretically (see Ref. [44] and references therein). Interestingly, a crucial dependence of the fcc versus hcp packing of small argon clusters on the number of the constituent atoms has been found in Refs. [45–49].

II. METHOD

The calculations have been performed within the *ab initio* Hartree-Fock (HF) method [50] as implemented in GAMESS [51]. Since the ground state of argon clusters with neutral thorium [see Figs. 1(b)–1(d)] has turned out to be a high spin (quintet) state, we have used the restricted open shell version of HF. The adopted molecular basis sets were 6-31G**, cc-pVDZ, aug-cc-pVDZ, and aug-cc-pVTZ [52] for argon, and the nonrelativistic all-electron augmented double zeta and triple zeta valence quality basis set with polarization functions jorge-ADZP and jorge-ATZP (abbreviated jADZP and jATZP) in the Basis Set Exchange site [53]) for thorium [54,55]. In general, the relativistic effects for actinides (including thorium) are important. However, in the scalar relativistic approach for valence electrons, one can work with effectively averaged radial components. As shown in Refs. [54,55], there are two ways to treat the problem: (1) Use the relativistic Douglas-Kroll-Hess (DKH) Hamiltonian, which is a preferred approach. However, in that case, one should also use relativistic basis sets for all other (even light) elements. Such relativistic calculations are usually performed for small molecules. (2) Use a nonrelativistic Hamiltonian for relatively large molecular complexes. Although this approach is not as precise as approach (1), the basis set of thorium is trained to correctly reproduce the essence of its chemical bonding. In the following, we adopt approach (2) to describe relatively large Th-Ar complexes. Note that unlike basis sets with the pseudopotential treatment of the core states, the jADZP and jATZP allow for a full core polarization effect of the thorium atom. To account for the correlations responsible for the weak dispersion forces in many cases, where available, we have used the second-order Møller-Plesset perturbation correction (MP2) [50]. Earlier, such an approach was applied to the bonding of neutral thorium to carbon nanomaterials [56].

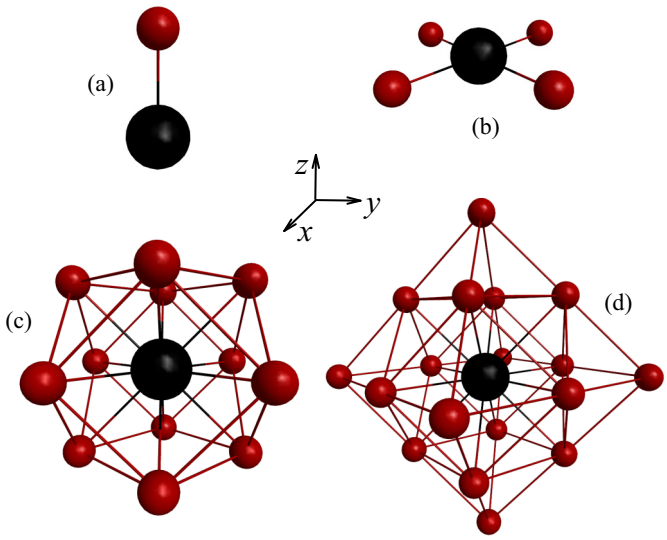

FIG. 1. (a) The ThAr diatomic molecule and clusters of thorium (black) with argon (red): (b) $ThAr_4$, (c) $ThAr_{12}$, and (d) $ThAr_{18}$, approximating the fcc lattice of solid argon.

III. RESULTS AND DISCUSSION

Argon as well as other rare gases are probably the most difficult elements to bind. According to Ref. [57], 1s and 2s2p electron shells of Ar quite effectively shield the nucleus and, as a result, the 3s3p shell is less contracted and extends to larger distances. When a chemical bond is formed, the 3s3p electron shell leads to a weak and shallow energy minimum that is very sensitive to such details of calculations as the basis set and method of calculations.

To better understand the nature of chemical bonding of Th in solid argon, we consider the ThAr diatomic molecule [Fig. 1(a)] and three different clusters [Figs. 1(b)–1(d)]: the thorium atom placed at the center of the square composed of four Ar atoms modeling four nearest neighbors lying in the xy, yz, or xz plane of solid argon [Fig. 1(b)], the thorium atom surrounded by 12 nearest neighbors ($ThAr_{12}$)—the first shell of the Ar atoms in the fcc lattice [Fig. 1(c)] and the thorium atom surrounded by 18 Ar atoms ($ThAr_{18}$) forming the first

TABLE I. Bond lengths for the molecule Ar_2 for various basis sets for Hartree-Fock (HF) and Hartree-Fock with MP2 (HF-MP2) calculations. D_e is the binding energy within HF-MP2.

Basis	6-31G**	cc-pVDZ	aug-cc-pVDZ	aug-cc-pVTZ
R_e, HF	4.513	4.513	4.746	4.956
R_e, HF-MP2	4.409	4.101	3.919	3.766
D_e (10^{-3} eV)	−0.67	−3.0	−11.24	−13.81

and second shells of the Ar atoms [Fig. 1(d)]. These cases are studied below in Secs. III B, III C, and III D, respectively.

To begin, however, in Sec. III A we investigate the chemical bonding in the simplest ThAr diatomic molecule, showing peculiarities of the binding between the thorium and argon atoms.

A. Chemical binding in Ar_2 and ThAr

We start with testing the Ar_2 dimer; see Table I. For both atoms lying along the z axis, the bonding proceeds through the polarization functions of the p_z-type, $p_z \sim Y_{l=1}^{m=0}$. (Here, $Y_{l=1}^{0}$, $Y_{l=1}^{m,c}$, and $Y_{l=1}^{m,s}$ are real spherical harmonics as defined in Ref. [58].) Since the p_z functions have relatively large radii, the resultant equilibrium bond length R_e between two Ar atoms is also large. Another crucial factor is a strong van der Waals force, which brings two argon atoms closer to each other. Within the Hartree-Fock approach, the van der Waals interaction is enabled through the second-order Møller-Plesset perturbation correction (MP2). From Table I, it follows that at the HF-MP2 level, the increase of the quality of the basis functions leads to smaller bond lengths, from 4.409 to 3.766 Å for aug-cc-pVTZ, which is very close to the experimentally deduced value of $R_e = 3.757$ Å [59]. It is worth mentioning that the Ar-Ar bond length in fcc argon, i.e., 3.748 Å [41], is only slightly smaller than the diatomic value. The calculated binding energy for Ar_2, $D_e = 13.81$ meV, overestimates the experimental one, $D_e^{\rm exp} = 12.34$ meV [59].

We next consider the ThAr diatomic molecule [Fig. 1(a)].

In that case, the bonding mechanism is completely different. The main characteristic is that it shows a strong dependence on total spin. Since the thorium atom has four valence electrons, the total spin takes the values $S = 0$ (singlet), $S = 1$ (triplet), or $S = 2$ (quintet). As shown in Fig. 2 and Table II, the ground state is realized for the high spin (quintet) state. Although the atomic thorium has the $6d^2 7s^2$ (^3F) open shell [60], its $5f$ electron can be easily promoted to participate in chemical bonding. (The $5f6d7s^2$ configuration of Th lies only 0.966 eV above the ground level [60].) This property of Th becomes apparent in considering the dependence of occupation of thorium orbitals on the spin state; see Table III. (Bader's charges [61] here and below are calculated with the MULTIWFN code [62]. The valence occupation of Th shown in Table III is obtained from the total Mulliken occupation by subtraction of the fully occupied core states.) The main difference is that in the ground high spin state, there is approximately one $5f$ electron, whereas for excited states with $S = 0$ or $S = 1$, there are two. The effective charge of thorium is also changed—from the small positive for the quintet state to that close to zero for the singlet state. Even the character of

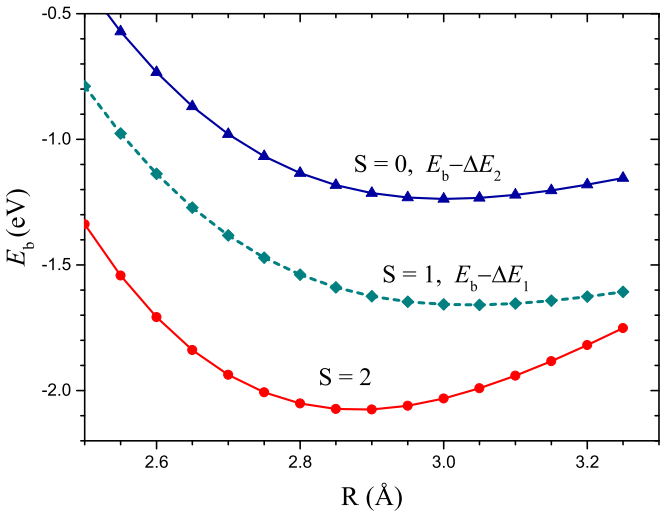

FIG. 2. Binding energy E_b (in eV) for the ThAr molecule as a function of the bond length R (in Å) for the spin quintet ($S = 2$), triplet ($S = 1$), and singlet ($S = 0$) states obtained with the aug-cc-pVTZ basis set for Ar and jorge-ATZP for Th. The excited spin triplet and singlet plots are shifted to lower energies by $\Delta E_1 = 1.6$ eV and $\Delta E_1 = 3.6$ eV, respectively.

the valence molecular orbitals (MOs) changes with S. In the ground quintet state, the occupied $5f$ states of thorium [with the $Y_{l=3}^{2,c} \sim (x^2 - y^2)z$ angular dependence] are found mainly in the molecular orbital MO2 (Fig. 3), while in the singlet and triplet states, they are found in the low-lying MO1. In the quintet state, MO1 is formed from the s states of Ar and s, $p_z \sim Y_{l=1}^{0}$, and d states ($Y_{l=2}^{0} \sim 3z^2 - 1$) of thorium.

In Fig. 2, we illustrate the binding energy of ThAr as a function of the bond length R, defined as

$$E_b(R) = E(R) - E(R_\infty), \tag{1}$$

where $E(R_\infty)$ is the lowest energy of the constituent elements at large distances. In our case, it corresponds to the quintet state of Th. (In practice, we take $R_\infty = 20$ Å.) The dissociation (binding) energy $D_e = E_b(R_e)$ at the equilibrium bond length R_e [minimum of $E_b(R)$] is quoted in Tables I and II, and others. A general scheme for the formation of chemical

TABLE II. Bond lengths R_e for the molecule ThAr for the Hartree-Fock (HF) and Hartree-Fock with MP2 (HF-MP2) calculations with various basis sets. D_e is the binding energy within HF-MP2.

Basis (Th)	jADZP	jADZP	jATZP
Basis (Ar)	6-31G**	cc-pVDZ	aug-cc-pVTZ
	Singlet spin state ($S = 0$)		
R_e, HF	4.580	3.044	3.016
R_e, HF-MP2	4.462	2.930	3.004
D_e (eV)	−0.068	3.246	2.444
	Quintet spin state ($S = 2$)		
R_e, HF	4.632	4.781	2.923
R_e, HF-MP2	4.604	4.564	2.881
D_e (eV)	−0.051	−0.034	−2.076

TABLE III. Occupation of valence states of thorium and its Bader's charges in ThAr for the HF-MP2 calculation with the jATZP(Th)/aug-cc-pVTZ(Ar) basis set.

	Spin	Config.	Q(Th)
Singlet	0	$p^{0.16}d^{1.99}f^{2.00}$	+0.021
Triplet	1	$s^{0.96}p^{0.95}d^{0.35}f^{1.98}$	+0.066
Quintet	2	$s^{0.93}p^{0.26}d^{1.64}f^{1.06}$	+0.116

bonding, which also holds for other cases considered in this work, is further illustrated in Fig. 3.

It is worth noting that for ThAr, the equilibrium bond length is approximately the same at the HF and HF-MP2 level of calculations; see Table II and Fig. 2.

B. Chemical bonding of the square group $ThAr_4$

In this section, we consider the thorium atom located at the center of the square of four argon atoms with the D_{4h} point symmetry [Fig. 1(b)]. In a fcc lattice, such four argon neighbors have coordinates $(\pm a/2, \pm a/2, 0)$ and lie in the xy plane, where a is the fcc lattice constant. Analogously, four argon neighbors can be chosen in the yz or xz plane.

The calculated equilibrium Th-Ar distances for different basis sets and corresponding binding energies are quoted in Table IV. The nature of the $ThAr_4$ chemical bonding is different from that of ThAr. In $ThAr_4$, s- and p-valence states of Th become active, whereas f states of Th practically do not participate in it. As a result, the averaged (Mulliken) configuration of thorium with the jATZP(Th)/aug-cc-pVTZ(Ar) basis is $s^{0.92}p^{0.68}d^{2.44}$ in the spin quintet state and $s^{1.62}p^{0.68}d^{2.26}$ in the spin singlet state. Bader's charges of thorium in these states are $Q(\mathrm{Th}) = +0.244$ and $+0.235$, correspondingly, and the charge transfer from Th to Ar is practically the same.

As in the ThAr diatomic molecule, in $ThAr_4$ the high spin state lies lower in energy than the low spin singlet one, but now the energy difference is much smaller, reaching only 1.078 eV.

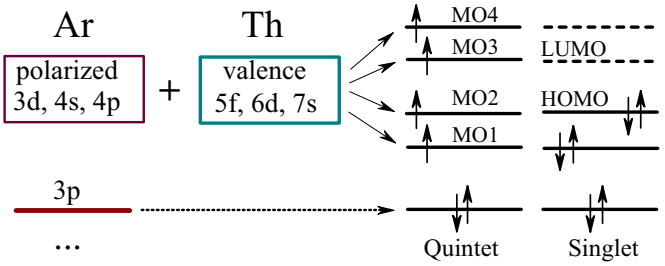

FIG. 3. Chemical bonding and valence molecular orbitals (MO1–MO4) in ThAr and other clusters of Th. In the high spin quintet state, MO1–MO4 are involved. In the low spin singlet state, MO2 corresponds to the highest occupied molecular orbital (HOMO) and MO3 corresponds to the lowest unoccupied molecular orbital (LUMO). In MO1–MO4, the contribution of polarized functions of argon is small. The state below MO1 (HOMO-2) belongs to $3p$ states of argon.

TABLE IV. Th-Ar bond lengths d for the $ThAr_4$ (C_{4v}) molecular group for the Hartree-Fock (HF) and Hartree-Fock with MP2 (HF-MP2) calculations with various basis sets. D_e is the binding energy within HF-MP2.

Basis (Th)	jADZP	jADZP	jATZP
Basis (Ar)	cc-pVDZ	aug-cc-pVDZ	aug-cc-pVTZ
		Singlet spin state ($S = 0$)	
d, HF	3.709	3.889	2.951
d, HF-MP2	2.839	3.839	2.837
D_e (eV)	−1.162	−1.420	−3.851
		Quintet spin state ($S = 2$)	
d, HF	3.744	3.831	2.935
d, HF-MP2	3.588	3.790	2.844
D_e (eV)	−2.657	−3.444	−4.929

C. Th surrounded by first nearest shell of Ar atoms of the fcc lattice ($ThAr_{12}$)

We next consider the thorium atom surrounded by 12 argon atoms constituting the first atomic shell of the fcc lattice of solid argon. At this stage, we keep the O_h cubic point group symmetry, while a possible symmetry lowering will be considered in Sec. III D. Results of the calculations are given in Table V.

As in the case of ThAr and $ThAr_4$, the chemical bonding between Th and 12 argon atoms is more favorable for the high spin quintet state. The energy difference is 1.083 eV for the jDZ(Th)/cc-pVDZ(Ar) basis set, and 6.855 eV for jDZ(Th)/aug-cc-pVDZ(Ar). As will be shown in the next section, the high spin quintet state remains being the ground state even if the symmetry of the thorium cluster is reduced.

In $ThAr_{12}$, the $4f$ and $7p$ states of Th are excluded from the bonding. Calculations show that for the jADZP(Th)/aug-cc-pVDZ(Ar) basis, the quintet ground state configuration of Th is $s^{1.66}d^{2.99}$, whereas the singlet one is $s^{0.15}d^{3.75}$. In the last case, the configuration of thorium becomes close to d^4. However, from the first Hund's rule, it follows that the energy of four d electrons is lower in a high spin state, where the Coulomb repulsion between the equivalent electrons is

TABLE V. Th-Ar bond length d and the binding energy (D_e, HF-MP2) for the $ThAr_{12}$ cluster of the O_h symmetry modeling the first atomic shell of the fcc lattice. Hartree-Fock (HF) and Hartree-Fock with MP2 (HF-MP2) calculations for the jADZP basis set for Th and various basis sets of Ar.

Basis (Ar)	6-31G**	cc-pVDZ	aug-cc-pVDZ
		Singlet spin state ($S = 0$)	
d, HF	3.841	4.034	3.510
d, HF-MP2		3.846	3.411
D_e (eV)		0.171	−1.139
		Quintet spin state ($S = 2$)	
d, HF	4.182	4.469	3.688
d, HF-MP2	4.100	4.144	3.531
D_e (eV)	−1.236	−0.912	−7.994

TABLE VI. Bond lengths ($d_{\min}$, d_{av}), the cluster binding energy (D_e), and effective charges of the neutral ($ThAr_{18}$) and charged ($Th^{n+}Ar_{18}$, $n = 1, 2, 3, 4$) thorium impurity in a deformed argon cluster of the D_{2h} symmetry. $d_{\min}$ is the smallest bond length between Th and neighboring Ar atoms, d_{av} is the averaged Th-Ar bond length, Q(Th) is the Bader charge [61] of thorium, and Q_{av}(Ar) is the averaged Bader charge of the neighboring argon (in e). Results of the Hartree-Fock (HF) calculations with the jADZP(Th)/aug-cc-pVDZ(Ar) basis sets.

Impurity	S	$d_{\min}$	d_{av}	D_e (eV)	Q(Th)	Q_{av}(Ar)	Val. conf. (Th)
Th	0	3.161	3.727	−8.499	0.308	−0.024	$s^{0.3}d^{5}$
Th	2	3.233	3.779	−9.030	0.284	−0.023	$s^{0.2}d^{4.3}$
Th^{+}	1/2	3.054	3.680	−5.009	1.121	−0.010	$s^{0.3}d^{1.4}f^{1.9}$
Th^{+}	3/2	3.154	3.703	−11.093	1.028	−0.003	$s^{0.3}d^{3.2}$
Th^{2+}	0	3.036	3.527	−9.507	1.863	+0.010	$s^{0.3}d^{0.2}f^{1.9}$
Th^{2+}	1	3.056	3.554	−13.817	1.849	+0.012	$s^{0.3}d^{1.3}f^{1}$
Th^{3+}	1/2	3.124	3.141	−21.503	2.605	+0.031	$s^{0.3}p^{0.1}d^{0.2}f^{1.0}g^{0.1}$
Th^{4+} (ortho)	0	3.054	3.054	−25.302	3.225	+0.062	$s^{0.3}p^{0.1}d^{0.6}g^{0.2}$
Th^{4+} (cubic)	0	3.100	3.100	−24.248	3.243	+0.059	$s^{0.3}p^{0.1}d^{0.2}g^{0.2}$

minimized. These considerations explain why the high spin state of thorium is preferable.

The bonding mechanism involves mainly the orbital d functions of Th, which belong to the E_g irreducible representation of the O_h group (i.e., $Y^{0}_{l=2} \sim 3z^2 - r^2$ and $Y^{2,c}_{l=2} \sim x^2 - y^2$). From argon, it is the same type of d orbitals, but in Ar, those are polarization functions whose partial weight is quite small.

From Table V, it also follows that in the best basis, the Th-Ar bond length in a cubic environment is 3.53 Å, which is only slightly smaller than the Ar-Ar bond length in the fcc lattice of solid argon. Therefore, solid argon is a material which can easily incorporate the neutral thorium atom into its lattice.

D. Two nearest shells of Ar atoms: $ThAr_{18}$ and charged clusters $Th^{n+}Ar_{18}$ (n = 1–4)

In this section, we consider displacements of argon atoms from the cubic symmetry to the D_{2h} point symmetry in the $Th^{n+}Ar_{18}$ cluster, where Th is the neutral atom ($n = 0$) or cation ($n = 1, 2, 3, 4$). We have not chosen the lowest symmetry because it would lead to a strongly deformed cluster. Such a situation, however, is not realistic because the other argon atomic shells would act as a restoring force trying to keep the fcc structure of solid argon. From that point of view, the choice of the D_{2h} symmetry is a compromise which, on one hand, requires a symmetry lowering, but, on the other hand, does not allow very large deformations from the fcc structure. In comparison with the previous section, we add the second shell consisting of six argon atoms located initially at $(\pm a, 0, 0)$, $(0, \pm a, 0)$, and $(0, 0, \pm a)$ sites of fcc. Thus, the total number of argon atoms becomes 18, with one atom of thorium at the (0,0,0) site [Fig. 1(d)]. In the $ThAr_{18}$ cluster, we allow for symmetry lowering from the cubic symmetry to orthorhombic (D_{2h}) and optimize the positions of all Ar atoms.

The obtained results of the HF calculations are summarized in Table VI for the jADZP(Th)/aug-cc-pVDZ(Ar) basis sets. The averaged bond length between thorium and the 12 closest argon atoms (d_{av}) in the $ThAr_{18}$ and $Th^{+}Ar_{18}$ cluster is very close to the Ar-Ar bond length in solid argon (3.75 Å). In $Th^{n+}Ar_{18}$ with $n = 2, 3, 4$, d_{av} is systematically reduced with n, implying a stronger bonding between the thorium cation and its neighbors. This conclusion is further confirmed by the concomitant increase in the absolute value of chemical bonding E_b with the increase of n from one to four; see Table VI. At first sight, this result is in contradiction with the expectation that the decreasing population of bonding molecular orbitals results in a weakening of chemical bonding. However, as pointed out earlier (Fig. 3), the Th-Ar bonding requires valence states of thorium and polarization states of argon. In such a system, there is a strong Coulomb repulsion between the occupied $3p$ states of Ar and the $6d7s5f$-valence shell of Th. Depopulation of the thorium valence states leads to a weakening of the repulsion. As a result, thorium moves closer to argon, thereby increasing its polarization. The increase of electron density on polarized argon orbitals and a better overlap with the valence and polarized orbitals of thorium imply a stronger bonding between Ar and Th. We have also analyzed MOs whose energies lie in the gap of forbidden states of solid argon; see Table VII. Although formally each MO is constructed from both thorium and argon states, in practice, due to its dominant contribution, it can be easily identified either with argon or thorium electron states. For example, in MO with the energy E_o(Ar, $3p$) (see Table VII and Fig. 3), the contribution of argon states for various Th ions

TABLE VII. Electron states of the Th impurity located in the energy gap of solid argon modeled with $Th^{n+}Ar_{18}$. E_o(Ar, $3p$) and E_v(Ar, $3p$) are the energy of the highest occupied and the lowest unoccupied MO ascribed to the top of the valence band and the bottom of the conducting band of solid Ar, respectively, E_g is the energy gap of Ar, E(α-HOMO,Th) is the highest occupied (α)MO of Th, and E_1(Th) and E_2(Th) are the lowest and the highest energy of the (α)MO of Th in the energy gap.

S	Th 2	Th^{+} 3/2	Th^{2+} 1/2
E_o(Ar, $3p$)	−15.192	−18.071	−20.645
E_v(Ar, $3p$)	2.286	−0.275	−3.037
E_g(Ar)	17.478	17.796	17.609
E(α-HOMO,Th)	1.434	−4.501	−8.014
E_1(Th)	0.231	−5.222	−9.753
E_2(Th)	1.434	−1.116	−3.976

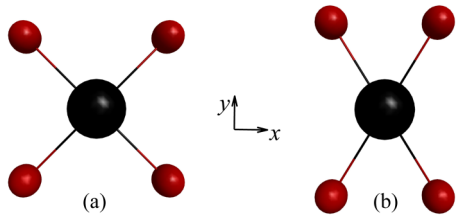

FIG. 4. Schematic difference between two different equilibrium geometries, (a) cubic and (b) orthorhombic, found for the $Th^{4+}Ar_{18}$ cluster and shown for four nearest neighbors of the Th^{4+} cation in the xy plane.

is typically 99.7% to 99.9%, whereas in MOs in the energy gap, the contribution of thorium states lies from 85% to 99%. (For these estimations, we have used Bader's partitioning of atomic space in molecules [61,62].) A small admixture of argon states in the gap indicates that the radiation decay of the Th isomeric state will not be suppressed. In comparison with the experimental data of the Ar energy gap [38–40], the calculated value of E_g in Th-Ar clusters is overestimated by ~50%. (In a pure Ar cluster, $E_g = 18.2$ eV.) This is partly due to the quality of the chosen basis set and partly due to the poor description of excited states in HF.

It is worth noting that for the Th^{4+} cation, there are no occupied valence states of thorium and the HOMO level is formed mainly by $3p$ states of argon. In that case, the bonding between thorium and its neighbors is caused by polarization effects from both argon atoms and the thorium cation and becomes highly isotropic. Indeed, our calculations in the end of the geometry optimization yield a highly symmetric cubic arrangement of argon atoms around Th^{4+} (last row of Table VI) when all bond lengths are equal. Nevertheless, the global energy minimum corresponds to another conformation of orthorhombic symmetry, shown in Fig. 4 for the arrangement of neighboring atoms in the xy plane. In that geometry, all bonds between the thorium cation and neighboring argon atoms being equal in length, deviate from the face-centered-cubic directions.

IV. CONCLUSIONS

We have studied the nature of chemical bonding between thorium and argon atoms in ThAr, $ThAr_4$, $ThAr_{12}$, and $ThAr_{18}$ and also in charged clusters $Th^{n+}Ar_{18}$, where $n = 1, 2, 3, 4$ (Fig. 1). Our aim was to model the bound states of a neutral thorium atom and thorium cations in solid (fcc) argon. Twelve argon atoms in $ThAr_{12}$ and 18 argon atoms in $ThAr_{18}$ represent one and two shells of nearest atoms around the thorium impurity in the fcc lattice. Calculations have been carried out within the restricted open shell Hartree-Fock approach, describing the high and low spin states of the thorium impurity. In addition, where available, we have used the MP2 correction to account for van der Waals forces.

We have found that the chemical bonding between Th and Ar for $n = 0, 1, 2, 3$ involves valence states of thorium and polarized states of argon (Fig. 3). In the ThAr diatomic molecule, the valence states are $6d$ and $5f$, in other clusters with the neutral thorium, they are mainly $6d$ and $7s$. In all cases where different spin quantum numbers are allowed (for example, for neutral thorium S can take the values of 0, 1, and 2), the ground state of the electron system adopts the highest spin configuration. For the neutral thorium atom, it is the spin quintet state ($S = 2$). This is a manifestation of the first Hund rule for the open mixed $6d$-$7s$-$5f$ electron shell of thorium. Lowering of the cubic symmetry to the orthorhombic (D_{2h}) one through the displacements of argon atoms in the $Th^{n+}Ar_{18}$ clusters ($n = 0, 1, 2$) keeps the high spin character of the ground state.

The character of chemical bonding and bond lengths in $Th^{n+}Ar_{18}$ are considered in detail in Sec. III D. In general, the calculated Th-Ar bond lengths for the Th and Th^+ impurity lie very close to the Ar-Ar bond lengths in solid argon, which suggests that solid argon can easily accommodate them in the argon lattice. For thorium cations Th^{n+}, our calculations show that the binding energy E_b grows, whereas the average bond length d_{av} decreases with the degree of ionization (n); see Table VI. We ascribe it to a decrease of repulsion between the Th cation and Ar and an increase of polarization of both Ar and Th^{n+}. The reduction of Th-Ar bond lengths for Th^{3+} and Th^{4+} results in a contraction of the lattice around these impurities.

In $Th^{4+}Ar_{18}$, there are no valence states of thorium and $S = 0$. In that case, the active orbitals are $3p$ from argon and polarized states from thorium. The quadruply ionized thorium being isotropic forms equal bonds with all argon neighbors; see Table VI. We have found two conformations of $Th^{4+}Ar_{18}$, i.e., the cubic and orthorhombic ones (Fig. 4), with the orthorhombic ground state lying 1.054 eV deeper in energy.

We finally remark on some practical aspects of the problem in view of the possible crystal damage effects. The question is how the α decay of the implanted ^{229}Th nuclei and the vacuum ultraviolet (UV) radiation affect the crystalline argon. In principle, the defects of the crystal structure appearing as a result of the α decay, and the external radiation heating can worsen the characteristics of the host crystal. These processes impose a number of strict requirements for the experiment, which we think can be satisfied by carrying out studies with a thin frozen argon film of thickness of about 100 nm deposited on the gold substrate [36] below the crystallization temperature. As follows from the direct measurements in the deposited frozen Xe films, even the influence of the xenon lamp resonance radiation with the power density of mW/cm^2 does not cause film melting or other structural changes [36]. The same applies to argon films. Due to the small film thickness, only a negligible fraction of the alpha particles from the implanted ^{229}Th nuclei is scattered in the film interior. Since the number of implanted ^{229}Th nuclei can reach 13^{13}–10^{14} per cm^2 [36] and the half life of ^{229}Th is 7880 yr, the alpha activity in the sample amounts to 10–100 Bq cm^{-2}. With the mean free path being dozens of micrometers, the fraction of alpha particles scattered by the film will be of the order of 10^{-3}. Thus, in the film area of 1 cm^2, the energy dissipation is caused only by one alpha particle per second, which should not damage the host crystal and should allow for successful measurements for at least a few hours.

The data that support the findings of this study are available from the corresponding author upon reasonable request.

ACKNOWLEDGMENTS

The authors thank Prof. N. Kolachevsky, Dr. P. Borisyuk, and Dr. Yu. Lebedinsky for helpful discussions of the problems considered in this paper. This research was supported by a grant of the Russian Science Foundation (Project No. 19-72-30014).

[1] J. Erler, N. Birge, M. Kortelainen, W. Nazarewicz, E. Olsen, A. M. Perhac, and M. Stoitsov, Nature (London) **486**, 509 (2012).

[2] E. Peik, T. Schumm, M. Safronova, A. Palffy, J. Weitenberg, and P. G. Thirolf, Quantum Sci. Technol. **6**, 034002 (2021).

[3] B. Seiferle, L. von der Wense, P. V. Bilous, I. Amersdorffer, C. Lemell, F. Libisch, S. Stellmer, T. Schumm, C. E. Dullmann, A. Palffy *et al.*, Nature (London) **573**, 243 (2019).

[4] T. Sikorsky, J. Geist, D. Hengstler, S. Kempf, L. Gastaldo, C. Enss, C. Mokry, J. Runke, C. E. Düllmann, P. Wobrauschek, K. Beeks, V. Rosecker, J. H. Sterba, G. Kazakov, T. Schumm, and A. Fleischmann, Phys. Rev. Lett. **125**, 142503 (2020).

[5] L. A. Kroger and C. W. Reich, Nucl. Phys. A **259**, 29 (1976).

[6] C. W. Reich and R. G. Helmer, Phys. Rev. Lett. **64**, 271 (1990).

[7] R. G. Helmer and C. W. Reich, Phys. Rev. C **49**, 1845 (1994).

[8] B. R. Beck, J. A. Becker, P. Beiersdorfer, G. V. Brown, K. J. Moody, J. B. Wilhelmy, F. S. Porter, C. A. Kilbourne, and R. L. Kelley, Phys. Rev. Lett. **98**, 142501 (2007).

[9] V. F. Strizhov and E. V. Tkalya, Sov. Phys. JETP **72**, 387 (1991).

[10] E. V. Tkalya, JETP Lett. **55**, 211 (1992).

[11] E. V. Tkalya, Sov. J. Nucl. Phys. **55**, 1611 (1992).

[12] P. Kalman and T. Keszthelyi, Phys. Rev. C **49**, 324 (1994).

[13] E. V. Tkalya, V. O. Varlamov, V. V. Lomonosov, and S. A. Nikulin, Phys. Scr. **53**, 296 (1996).

[14] S. G. Porsev, V. V. Flambaum, E. Peik, and C. Tamm, Phys. Rev. Lett. **105**, 182501 (2010).

[15] R. A. Muller, A. V. Volotka, and A. Surzhykov, Phys. Rev. A **99**, 042517 (2019).

[16] P. V. Borisyuk, N. N. Kolachevsky, A. V. Taichenachev, E. V. Tkalya, I. Y. Tolstikhina, and V. I. Yudin, Phys. Rev. C **100**, 044306 (2019).

[17] E. V. Tkalya, Phys. Rev. Lett. **120**, 122501 (2018).

[18] V. V. Flambaum, Phys. Rev. Lett. **97**, 092502 (2006).

[19] E. Litvinova, H. Feldmeier, J. Dobaczewski, and V. Flambaum, Phys. Rev. C **79**, 064303 (2009).

[20] J. C. Berengut, V. A. Dzuba, V. V. Flambaum, and S. G. Porsev, Phys. Rev. Lett. **102**, 210801 (2009).

[21] E. V. Tkalya, Phys. Rev. A **94**, 012510 (2016).

[22] M. S. Safronova, D. Budker, D. DeMille, Derek F. Jackson Kimball, A. Derevianko, and C. W. Clark, Rev. Mod. Phys. **90**, 025008 (2018).

[23] A. M. Dykhne and E. V. Tkalya, JETP Lett. **67**, 549 (1998).

[24] A. M. Dykhne, N. V. Eremin, and E. V. Tkalya, JETP Lett. **64**, 345 (1996).

[25] E. Peik and C. Tamm, Europhys. Lett. **61**, 181 (2003).

[26] W. G. Rellergert, D. DeMille, R. R. Greco, M. P. Hehlen, J. R. Torgerson, and E. R. Hudson, Phys. Rev. Lett. **104**, 200802 (2010).

[27] C. J. Campbell, A. G. Radnaev, A. Kuzmich, V. A. Dzuba, V. V. Flambaum, and A. Derevianko, Phys. Rev. Lett. **108**, 120802 (2012).

[28] E. Peik and M. Okhapkin, C. R. Phys. **16**, 516 (2015).

[29] E. V. Tkalya, Phys. Rev. Lett. **106**, 162501 (2011).

[30] E. V. Tkalya and L. P. Yatsenko, Laser Phys. Lett. **10**, 105808 (2013).

[31] E. V. Tkalya, Phys. Rev. Lett. **124**, 242501 (2020).

[32] E. V. Tkalya, JETP Lett. **71**, 311 (2000).

[33] E. V. Tkalya, A. N. Zherikhin, and V. I. Zhudov, Phys. Rev. C **61**, 064308 (2000).

[34] G. A. Kazakov, M. Schreitl, G. Winkler, J. H. Sterba, G. Steinhauser, and T. Schumm, arXiv:1110.0741.

[35] P. V. Borisyuk, E. V. Chubunova, Yu. Yu. Lebedinskii, E. V. Tkalya, O. S. Vasilyev, V. P. Yakovlev, E. Strugovshchikov, D. Mamedov, A. Pishtshev, and S. Zh. Karazhanov, Laser Phys. Lett. **15**, 056101 (2018).

[36] U. N. Kurelchuk, P. V. Borisuyk, E. V. Chubunova, S. Z. Karazhanov, N. N. Kolachevsky, Yu. Yu. Lebedinskii, D. A. Myzin, A. V. Nikolaev, and E. V. Tkalya (unpublished).

[37] J. Jeet, Ch. Schneider, S. T. Sullivan, W. G. Rellergert, S. Mirzadeh, A. Cassanho, H. P. Jenssen, E. V. Tkalya, and E. R. Hudson, Phys. Rev. Lett. **114**, 253001 (2015).

[38] R. S. Knox and F. Bassani, Phys. Rev. **124**, 652 (1961).

[39] K. Hashizume, J. Phys. Chem. Solids **48**, 153 (1987).

[40] M. Förstel, M. Mucke, T. Arion, T. Lischke, S. Barth, V. Ulrich, G. Öhrwall, O. Björneholm, U. Hergenhahn, and A. M. Bradshaw, Phys. Rev. B **82**, 125450 (2010).

[41] C. S. Barrett and L. Meyer, J. Chem. Phys. **41**, 1078 (1964).

[42] D. Errandonea, R. Boehler, S. Japel, M. Mezouar, and L. R. Benedetti, Phys. Rev. B **73**, 092106 (2006).

[43] Y. A. Freiman, A. F. Goncharov, S. M. Tretyak, A. Grechnev, J. S. Tse, D. Errandonea, H.-K. Mao, and R. J. Hemley, Phys. Rev. B **78**, 014301 (2008).

[44] B. Li, G. Qian, A. R. Oganov, S. E. Boulfelfel, and R. Faller, J. Chem. Phys. **146**, 214502 (2017).

[45] E. T. Verkhovtseva, I. A. Gospodarev, A. V. Grishaev, S. I. Kovalenko, D. D. Solnyshkin, E. S. Syrkin, and S. B. Feodosev, Low Temp. Phys. **29**, 386 (2003).

[46] O. G. Danylchenko, S. I. Kovalenko, and V. N. Samovarov, Low Temp. Phys. **30**, 166 (2004).

[47] A. G. Danilchenko, S. I. Kovalenko, and V. N. Samovarov, Low Temp. Phys. **34**, 966 (2008).

[48] O. G. Danylchenko, S. I. Kovalenko, O. P. Konotop, and V. N. Samovarov, Low Temp. Phys. **40**, 1083 (2014).

[49] N. V. Krainyukova, R. E. Boltnev, E. P. Bernard, V. V. Khmelenko, D. M. Lee, and V. Kiryukhin, Phys. Rev. Lett. **109**, 245505 (2012).

[50] A. Szabo and N. S. Ostlund, *Modern Quantum Chemistry* (McGraw-Hill, Dover, 1989).

[51] M. W. Schmidt, K. K. Baldridge, J. A. Boatz, S. T. Elbert, M. S. Gordon, J. H. Jensen, S. Koseki, N. Matsunaga, K. A. Nguyen, S. Su, T. L. Windus, M. Dupuis, and J. A. Montgomery, J. Comput. Chem. **14**, 1347 (1993).

[52] T. H. Dunning, Jr., J. Chem. Phys. **90**, 1007 (1989).

[53] Basis Set Exchange ver. 2, BSE Library v0.8.12, 2019. The Molecular Sciences Software Institute (MolSSI), Virginia Tech., https://www.basissetexchange.org
[54] L. S. C. Martins, F. E. Jorge, M. L. Franco, and I. B. Ferreira, J. Chem. Phys. **145**, 244113 (2016).
[55] A. Z. de Oliveira, C. T. Campos, F. E. Jorge, I. B. Ferreira, and P. A. Fantin, Comput. Theor. Chem. **1135**, 28 (2018).
[56] A. V. Bibikov, A. V. Nikolaev, and E. V. Tkalya, Phys. Chem. Chem. Phys. **22**, 22501 (2020).
[57] G. Frenking, W. Koch, F. Reichel, and D. Cremer, J. Am. Chem. Soc. **112**, 4240 (1990).
[58] C. J. Bradley and A. P. Cracknell, *The Mathematical Theory of Symmetry in Solids* (Clarendon, Oxford, 1972).
[59] J. F. Ogilvie and F. Y. H. Wang, J. Molec. Struct. **273**, 277 (1992).
[60] A. Kramida, Yu. Ralchenko, J. Reader, and NIST ASD Team (2020), NIST Atomic Spectra Database (ver. 5.8), https://physics.nist.gov/asd (National Institute of Standards and Technology, Gaithersburg, MD), doi:10.18434/T4W30F.
[61] R. F. W. Bader, *Atoms in Molecules: A Quantum Theory*, Intl. Ser. Mon. Chem. (Oxford University Press, Oxford, 1994).
[62] T. Lu and F. Chen, J. Comput. Chem. **33**, 580 (2012).